Developmental Cell
Article

Primitive Erythropoiesis Is Regulated by miR-126 via Nonhematopoietic Vcam-1$^+$ Cells

Christopher M. Sturgeon,[1] Laurie Chicha,[2] Andrea Ditadi,[1] Qinbo Zhou,[3] Kathleen E. McGrath,[5] James Palis,[5] Scott M. Hammond,[6] Shusheng Wang,[3] Eric N. Olson,[4] and Gordon Keller[1,*]
[1]McEwen Centre for Regenerative Medicine, University Health Network, Toronto, ON M5G1L7, Canada
[2]F. Hoffmann-la Roche, CNS Discovery Neuroregeneration Group, Basel 4070, Switzerland
[3]Department of Ophthalmology
[4]Department of Molecular Biology
University of Texas Southwestern Medical Center, Dallas 75390-9148, TX, USA
[5]Department of Pediatrics, Center for Pediatric Biomedical Research, University of Rochester Medical Center, Rochester, NY 14632, USA
[6]Department of Cell and Developmental Biology, University of North Carolina, Chapel Hill, NC 27514, USA
*Correspondence: gkeller@uhnresearch.ca
http://dx.doi.org/10.1016/j.devcel.2012.05.021

SUMMARY

Primitive erythropoiesis defines the onset of hematopoiesis in the yolk sac of the early embryo and is initiated by the emergence of progenitors assayed as colony-forming cells (EryP-CFCs). EryP-CFCs are detected for only a narrow window during embryonic development, suggesting that both their initiation and termination are tightly controlled. Using the embryonic stem differentiation system to model primitive erythropoiesis, we found that miR-126 regulates the termination of EryP-CFC development. Analyses of miR-126 null embryos revealed that this miR also regulates EryP-CFCs in vivo. We identified *vascular cell adhesion molecule-1* (*Vcam-1*) expressed by a mesenchymal cell population as a relevant target of miR-126. Interaction of EryP-CFCs with Vcam-1 accelerated their maturation to ßh1-globin$^+$ and Ter119$^+$ cells through a Src family kinase. These findings uncover a cell nonautonomous regulatory pathway for primitive erythropoiesis that may provide insight into the mechanism(s) controlling the developmental switch from primitive to definitive hematopoiesis.

INTRODUCTION

The onset of hematopoiesis in the yolk sac of the mouse embryo is characterized by the emergence of blood islands that are comprised of clusters of primitive erythroblasts surrounded by developing vascular cells (reviewed by Ferkowicz and Yoder, 2005). Primitive erythropoiesis represents a unique hematopoietic program in that its emergence is restricted to the yolk sac, and the progenitors assayed as colony-forming cells (EryP-CFCs) are present only during a defined temporal window early in mouse development (Palis et al., 1999). Studies using model organisms and the mouse embryonic stem cell (ESC) differentiation system have provided strong evidence that the primitive erythroid lineage derives from a Flk-1$^+$ mesodermal progenitor known as the hemangioblast (Choi et al., 1998; Huber et al., 2004; Nishikawa et al., 1998). The hemangioblast develops prior to the onset of primitive erythropoiesis and displays the capacity to generate both hematopoietic (including primitive erythroid) and vascular progeny (Choi et al., 1998). As observed in the yolk sac, primitive erythropoiesis in the mESC system represents a transient program that emerges following the development of the hemangioblast and persists for a defined period of time (Nostro et al., 2008; Palis et al., 1999). The striking similarities between yolk sac- and mESC-derived primitive erythropoiesis strongly support the notion that this in vitro model faithfully recapitulates hematopoietic development and, as such, provides a tractable system for investigating the regulation of this early blood cell program.

The temporal nature of primitive erythropoiesis points to tight controls regulating both the onset and the cessation of EryP-CFC production. Studies using the mESC model have provided important insights into signaling pathways that regulate the establishment of the lineage, including the induction of hematopoietic mesoderm and its specification to the primitive erythroid lineage. Findings from these studies have shown that BMP is essential for induction of Flk-1$^+$ mesoderm, whereas VEGF/Flk-1 signaling is required for specification of the mesoderm to the hematopoietic fates (Choi et al., 1998; Nostro et al., 2008; Pearson et al., 2008). Following hematopoietic specification, the primitive erythroid lineage is established through coordinated activation of the canonical Wnt pathway and inhibition of Notch signaling (Cheng et al., 2008). While these data provide a framework for the network of pathways that control the onset of primitive erythropoiesis, the termination of EryP-CFC development is poorly understood.

One class of regulators that could be involved in temporal regulation of primitive erythroid progenitor development is microRNAs, which function to silence genes by either translational repression or mRNA degradation (Bartel, 2004). To date, over 600 mouse microRNAs are annotated within the miRBase database (Griffiths-Jones, 2004), highlighting the potential of these molecules to regulate multiple stages of development and cell function across many cell lineages. Due to their

posttranscriptional regulation of target gene expression, microRNAs represent an ideal mechanism for controlling critical developmental stages in the embryo that involve the rapid induction and specification of distinct cell types in close proximity (reviewed in Kloosterman and Plasterk, 2006). An essential role for microRNAs in early development is demonstrated by the early lethality of embryos lacking Dicer, a nuclease essential for microRNA biogenesis (Bernstein et al., 2003). MicroRNAs have been shown to play multiple roles in the specification and function of different cell types, including those of the hematopoietic, cardiovascular, and neuronal systems (reviewed in Ivey and Srivastava, 2010).

In this study, we used mESC-derived cell populations to screen for potential microRNA(s) that could play a role in early hematopoietic development and identified miR-126 as a regulator of the primitive erythroid lineage. We found that inducible overexpression of miR-126 prolongs the duration of EryP-CFC development in the mESC model, whereas its targeted deletion has the opposite effect. miR-126 exerts these effects through the repression of *Vascular cell adhesion molecule-1* (*Vcam-1*) in a nonhematopoietic mesenchymal population. Vcam-1 regulates primitive erythropoiesis by accelerating maturation of primitive erythroblasts toward ßh1-globin expressing, $Ter119^+$ erythroid cells, via a Src-family kinase (SFK). Collectively, these findings define a cell nonautonomous regulatory pathway for primitive erythropoiesis involving miR-126, Vcam-1 and SFK.

RESULTS

miR-126 Is Expressed in a Yolk-Sac-like Population

To identify microRNAs that could play a role in early hematopoietic development, we performed microarray analysis to assess microRNA expression in mESC-derived populations representing distinct developmental stages in the pathway from the mESC to blood. Populations used for these analyses included epiblast-like cells prior to induction of a primitive streak (PS) population, *Brachyury*$^+$ and *Brachyury*$^+$*Foxa2*$^+$ cells representing a PS-like cell population, and cardiac and hematopoietic mesoderm generated from the PS cells. (Figure S1A available online). This screen identified microRNAs that were preferentially expressed at different stages of the developmental scheme including miR-302a and the miR-291–295 cluster in the PS-like population and miR-1 in cardiac mesoderm, consistent with published findings (Zhao et al., 2005; Figure S1B). miR-126-3p displayed an interesting pattern as its expression was upregulated with commitment to the hematopoietic and cardiac lineage (Figures S1B and S1C). Previous studies have shown that miR-126-3p is expressed in both vascular cells and hematopoietic progenitors (Donahue et al., 2009; Garzon et al., 2006; Gentner et al., 2010; Grabher et al., 2010; Harris et al., 2008, 2010; Jin et al., 2008; Kuehbacher et al., 2007; Lagos-Quintana et al., 2002; Landgraf et al., 2007; Li et al., 2008; Nicoli et al., 2010; O'Connell et al., 2010; Poliseno et al., 2006; Shen et al., 2008; Wienholds et al., 2005; Yang et al., 2009) and that it plays a role in vasculogenesis/vascular integrity (Fish et al., 2008; Wang et al., 2008). Given this expression pattern, we chose to further investigate the role of miR-126-3p in early hematopoietic development.

miR-126 Is Expressed in a VEGF-Dependent Manner in a Population Containing Primitive Erythroid Progenitors

Given the coincident upregulation of miR-126 with hematopoietic commitment, we were interested in determining if its expression was induced by one of the regulators of this developmental program. To address this, we generated a mESC reporter line containing a sensor to enable us to rapidly monitor miR-126 expression. A constitutively expressed tdRFP reporter containing two complementary binding sites to miR-126-3p in its 3′UTR (Luche et al., 2007; Mansfield et al., 2004) was inserted within the *ROSA26* locus (Figure 1Ai). Factors known to regulate the differentiation of mESCs to mesoderm (Gadue et al., 2006; Nostro et al., 2008; Pearson et al., 2008) were added to differentiation cultures, and tdRFP fluorescence was monitored temporally by flow cytometry (Figure 1Aii). None of the PS inducers, including Wnt3a, Activin A, or BMP4, reduced tdRFP fluorescence (Figure 1Aiii), indicating that they did not induce expression of miR-126. In contrast, addition of VEGF resulted in a loss of tdRFP beginning at day 5 of differentiation, demonstrating that signaling through the Flk-1 receptor induces functional miR-126-3p expression (Figure 1Aiii).

Titration of VEGF showed that induction of miR-126-3p (loss of tdRFP) and hematopoietic specification as measured by upregulation of CD41 expression are coordinated and require similar levels of signaling (Figure 1B). Kinetic analyses of mESC-derived populations induced with Wnt3a, BMP4, Activin A, and VEGF in serum-free conditions revealed a defined temporal pattern of primitive erythropoiesis, with EryP-CFCs emerging at day 4 of differentiation, peaking in number at day 5 and showing a rapid decline by day 6 (Figure 1C; Nakano et al., 1996; Nostro et al., 2008; Palis et al., 1999). Expression of miR-126-3p and its host gene, *Egfl7*, were upregulated with the onset of primitive erythropoiesis at day 4 of differentiation and maintained for the duration of the timecourse (Figures 1D, S2A, and S2B, black bars). To determine if expression of miR-126-3p changed as the primitive erythroid lineage matured, EryP-CFCs were cultured under serum-free conditions known to support their maturation and assayed and analyzed at daily intervals. Within 24 hr of erythropoietin (EPO) exposure in methylcellulose, miR-126-3p, and *Egfl7* expression dropped significantly and remained low throughout the 5 days of culture (Figures 1E and S2I), indicating that expression is not maintained during maturation of the primitive erythroid lineage.

Enforced miR-126 Expression in Differentiating EBs Alters Primitive Erythropoiesis through a Flk-1$^+$ Progenitor

To investigate a potential role for miR-126 in hematopoietic development, we engineered the AINV mESC line to allow *tet*-inducible miR-126 expression (Figure 2A; Kyba et al., 2002). With this line, expression of the gene of interest can be induced at any stage of differentiation by the addition of doxycycline (DOX) to the culture. Induction at early stages of differentiation (days 0–4) prior to endogenous expression of miR-126 resulted in a substantial decrease in total EB cell number and poor differentiation (data not shown). Overexpression in the methylcellulose EryP-CFC assay was also inhibitory and resulted in poor colony growth (Figure S2J), consistent with the downregulation

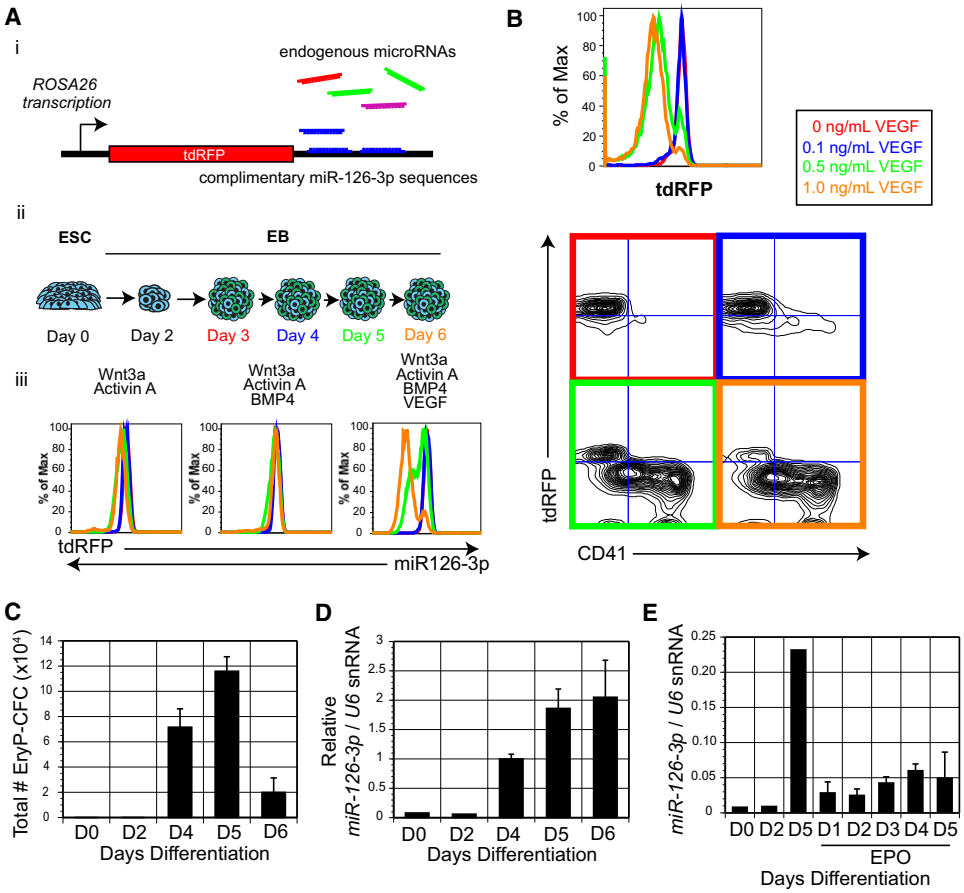

Figure 1. Induction of Expression of miR-126-3p

(A) Scheme showing the mESC line carrying a targeted miR-126-3p endogenous expression sensor. (i) *tdRFP* with two complimentary miR-126-3p sequences in the 3′UTR was placed under control of the *ROSA26* promoter. (ii) Differentiation schematic for monitoring endogenous miR-126-3p expression. Differentiated mESCs were reaggregated after 48 hr and further differentiated in the presence of indicated factors. Induced populations were assayed via flow cytometry for tdRFP fluorescence every 24 hr for 96 hr. Day 3, red; day 4, blue; day 5, green; day 6, orange.

(B) Endogenous miR-126-3p expression correlates with hematopoietic surface marker expression. Increasing concentrations of VEGF were added to sorted D3.5 Flk-1^{+} cells, and CD41 expression was monitored alongside tdRFP via flow cytometry 48 hr later.

(C and D) Kinetics of EryP-CFC development (C) and miR-126-3p expression in EBs (D).

(E) miR-126-3p is expressed in the EryP-CFC progenitor pool, but not maturing erythroblasts. EryP-CFC containing cells from day 5 of differentiation (C) were plated in methylcellulose, harvested every 24 hr as primitive erythroid colonies emerge, and quantified for miR-126-3p expression. n ≥ 3 (mean ± SD).

See also Figure S1.

of expression in maturing erythroid colonies (Figure 1E). These observations highlight the importance of manipulating microRNA expression levels at appropriate stages in developmental models.

Addition of DOX to differentiating EBs at day 4 of culture (Figure 2A) resulted in a 4-fold increase in miR-126-3p expression by day 6 (Figure S2A). Induction of miR-126 did not alter *Egfl7* expression (Figure S2B) nor did it affect cell proliferation, because total cell numbers in the induced and noninduced EBs were the same (Figure S2C). miR-126 overexpression did result in a striking 4-fold increase in the frequency and total number of EryP-CFCs detected in day 6 EBs (Figures S2D and 2B). Interestingly, this increase was not observed at day 5, suggesting that the effect is restricted to the termination of the primitive progenitor development. Regardless of miR-126 expression levels, however, the effect on primitive erythropoiesis did not persist to day 7 of differentiation as only low numbers of EryP-CFC were detected in all cultures (data not shown).

To determine if a loss of miR-126-3p would have an opposite effect on EryP-CFC development, we generated a miR-126$^{-/-}$ mESC line by targeting the second allele in the miR-126$^{+/-}$ heterozygous cell line (Wang et al., 2008). Analyses of these EBs showed that miR-126-3p was not detectable at any stage of differentiation (Figure S2A′), whereas *Egfl7* expression was slightly elevated (Figure S2B′). Cellular proliferation was unchanged between miR-126$^{-/-}$ and miR-126$^{+/-}$ EBs (Figure S2C′). Loss of miR-126 significantly impacted primitive erythropoiesis as day 6 EBs generated from the miR-126$^{-/-}$ cells showed more than a 2-fold reduction in total EryP-CFCs compared to miR-126$^{+/-}$-derived EBs (Figures 2C and S2D′). Myeloid progenitor numbers were not reduced in the miR-126$^{-/-}$ EBs (Figure S2E), demonstrating that the effect is

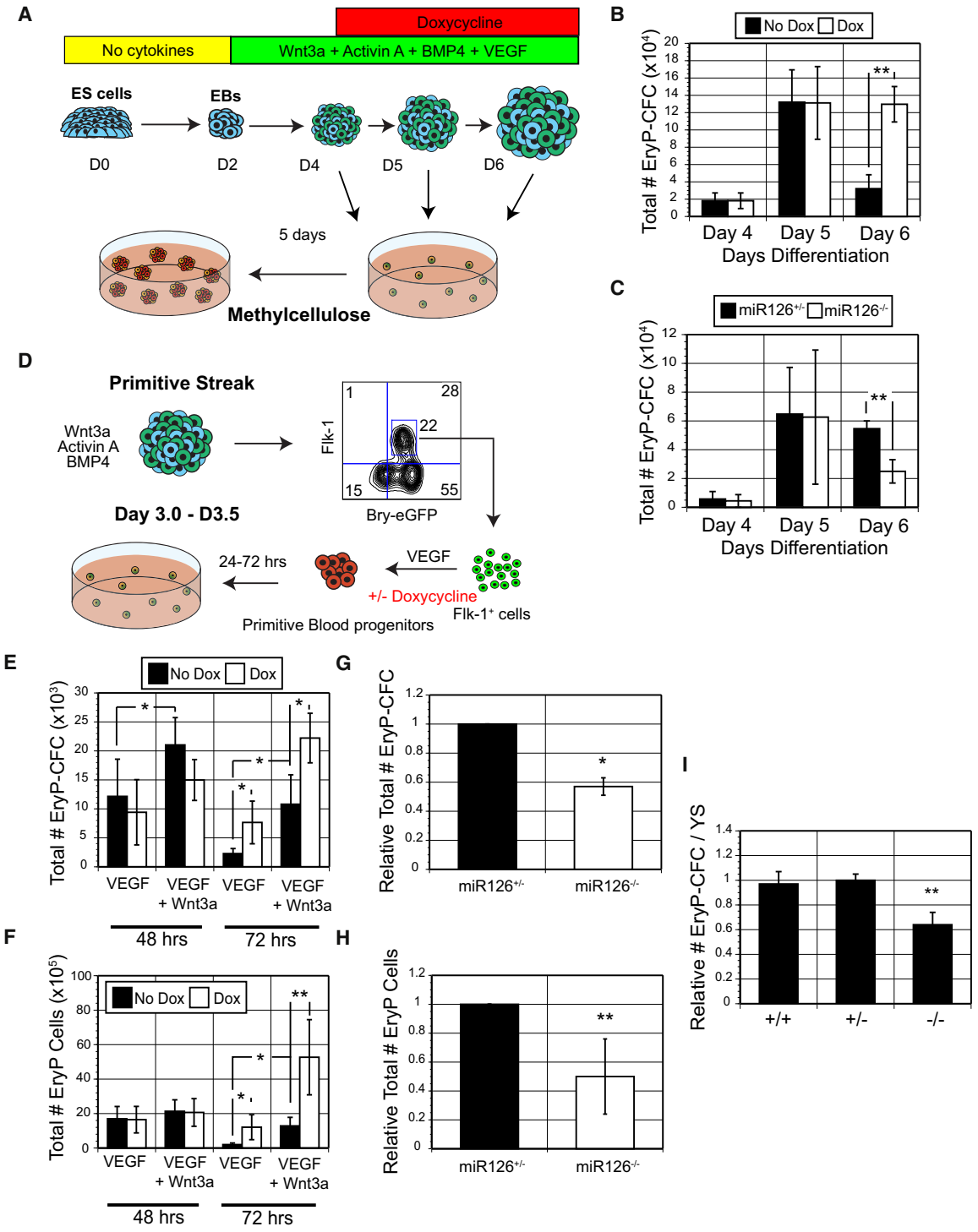

Figure 2. Manipulation of miR-126 Expression Alters Flk-1-Derived Primitive Erythroid Potential

(A) Differentiation scheme for monitoring EryP-CFCs potential following induction of miR-126 expression. Doxycycline (DOX; 2 μg/ml) was added to the EBs at day 4 of culture. EBs harvested on the day of DOX addition, or 24 and 48 hr later, were dissociated by trypsinization and the cells were plated in methylcellulose for EryP-CFC analysis.

(B) Total numbers of EryP-CFCs in induced and noninduced cultures.

(C) Total numbers of EryP-CFCs in cultures generated from miR-126$^{+/-}$ and miR-126$^{-/-}$ mESCs.

(D) Differentiation scheme outlining the strategy for the generation, isolation, and differentiation of the Flk-1^{+} progenitor population.

(E and F) Total number of EryP-CFCs in Flk-1^{+}-derived aggregates cultured for 2 days (48 hr) or 3 days (72 hr) following addition of DOX, and (F) total number of primitive erythroblasts generated from the EryP-CFCs in (E).

restricted to the primitive erythroid lineage. As with the enforced expression studies, the effect was only observed at day 6 of differentiation, further supporting the interpretation that miR-126 does not play a role in the initiation of primitive erythropoiesis, but rather is involved in the termination of EryP-CFC production.

The observation that VEGF controls miR-126 expression suggests that the effect on primitive erythropoiesis may be mediated via a Flk-1$^+$ progenitor, possibly through derivative hematopoietic, endothelial, or vascular cell-types (Choi et al., 1998; Kennedy et al., 1997). To investigate this possibility, we isolated the Flk-1$^+$ (hemangioblast) population from day 3.0–3.5 Wnt3a/Activin/BMP4 induced EBs, aggregated the cells in the presence of VEGF, and cultured the aggregates for an additional 3 days (Figure 2D). As with the whole EB population, VEGF induced miR-126-3p and *Egfl7* expression in a dose-dependent fashion (Figure S2F) and the expression was maintained for at least 72 hr (Figure S2G).

Peak numbers of EryP-CFCs were detected within 48 hr of culture after which time they declined sharply, indicating that these progenitors display a temporal pattern of development in the Flk-1$^+$-derived aggregates, similar to that observed in whole EBs. As expected from our previous study (Nostro et al., 2008), addition of Wnt3a to the aggregate cultures increased progenitor numbers at both time points but did not significantly alter the overall pattern of development (Figure 2E). Enforced overexpression of miR-126 at the onset of culture (day 3.0) did not affect proliferation of Flk-1$^+$ cells or hemangioblast potential of the population as measured by blast colony-forming cells (Figure S2H). miR-126 expression was also unable to induce primitive erythropoiesis in the absence of VEGF (data not shown). Induced expression did, however, result in 3.3- and 2.1-fold increases in the total EryP-CFC number at 72 hr in the VEGF- and VEGF+Wnt3a-stimulated cultures, respectively (Figure 2E). Furthermore, colonies generated from the induced populations were approximately 2-fold larger in size compared to those that developed from the noninduced progenitors (not shown), translating to a 6- and 4-fold increase in total numbers of primitive erythroblasts generated in the VEGF- or VEGF+Wnt3a-stimulated cultures (Figure 2F). As expected from the whole EB studies, miR-126$^{-/-}$ Flk-1$^+$ aggregates stimulated with VEGF and Wnt3a for 72 hr generated significantly fewer EryP-CFCs (43%) and total primitive erythroblasts (50%) compared to the miR-126$^{+/-}$ Flk-1$^+$ cells (Figures 2G and 2H).

To determine if miR-126 regulates primitive erythropoiesis in vivo, we next analyzed the yolk sacs from miR-126 null embryos (Wang et al., 2008) for EryP-CFCs. As observed with the miR-126$^{-/-}$ EBs, yolk sacs from miR-126$^{-/-}$ embryos contained significantly fewer EryP-CFCs than yolk sacs from the miR-126$^{+/-}$ embryos (Figure 2I; Table S1). Similar numbers of EryP-CFCs were detected in the miR-126$^{+/-}$ and miR-126$^{+/+}$ yolk sacs.

Collectively, these findings provide strong evidence that miR-126 plays a regulatory role in the termination of primitive erythropoiesis and that this effect is mediated within the Flk-1$^+$ hemangioblast-derived population.

miR-126-3p Regulates *Vcam-1* Expression on Nonhematopoietic Cells, Which Regulate EryP-CFC Potential

In the *tet*-inducible and targeted cell lines, both miR-126-3p and miR-126-5p are experimentally modulated (Figure S3A). Therefore, in order to define the targets regulated by miR-126 that could be responsible for the effects on the primitive erythroid lineage, we chemically modulated miR-126-5p or -3p expression independently using antagomirs (Krützfeldt et al., 2005). Inhibition of miR-126-3p, but not miR-126-5p, resulted in a 40% reduction of EryP-CFC in reaggregated Flk-1$^+$ cells (Figure S3B), indicating that miR-126-3p, and not -5p, is responsible for the observed regulatory effects on the primitive erythroid program.

qRT-PCR analysis of recently published targets of miR-126-3p, including *Ptpn9*, *Spred1*, and *Pi3kr2*, excluded them as potential targets for the primitive erythroid effect as their expression patterns in different aged EBs were not influenced by the absence of miR-126-3p or by its enforced expression (Figures S3C and S3D and data not shown). *Vcam-1*, on the other hand, was identified as a candidate target in the day 6 EB population (Harris et al., 2008). Kinetic analysis of whole EBs revealed that *Vcam-1* expression levels increased significantly between days 5 and 6 of differentiation, coincident with the decline in primitive erythropoiesis observed at the end of the program (Figure 3A). Expression levels at day 6 were reduced (37%) in DOX-induced day 6 EBs compared to non-treated control EBs, whereas they were 2.3-fold higher in miR-126$^{-/-}$ EBs than in miR-126$^{+/-}$ EBs (Figures 3A and 3B). These changes were also observed at the protein level as DOX-treated day 6 EBs contained fewer Vcam-1^{high} cells than noninduced EBs, whereas the miR-126$^{-/-}$ EBs had a larger Vcam-1^{high} population than the corresponding miR-126$^{+/-}$ EBs (Figure 3C).

To determine if Vcam-1(CD106) is a regulator of primitive erythropoiesis, we antagonized its expression through inducible expression of a shRNA against *Vcam-1* using the tet-inducible AINV mESC line. Screening for functional shRNA against *Vcam-1* indentified 1 clone wherein stably-transfected mESC were differentiated and assayed for primitive erythropoiesis as in Figure 2A. shRNA against *Vcam-1* decreased Vcam-1 expression by 25% (Figure S3E) and increased total EryP-CFCs by 2-fold (Figure S3F). DOX induction of the same Vcam-1 shRNA at day 4 of differentiation resulted in a 2.3-fold reduction in the size of Vcam-1^{high} population (Figure 3D) and a comparable (2.3-fold) increase in the total number of EryP-CFCs at day 6 of differentiation (Figure 3E). Similarly, DOX induction in day 3.0 Flk-1$^+$-derived aggregates decreased Vcam-1 expression (Figure S3G) and resulted in 3.3- and 2.3-fold increases in total EryP-CFCs in VEGF- and VEGF+Wnt3A-induced reaggregates (Figure S3H). The increase in total primitive erythroblasts was 4.5-fold and 2.1-fold for the VEGF- and VEGF+Wnt3a-treated

(G) Total number of EryP-CFC generated in miR-126$^{+/-}$ and miR-126$^{-/-}$ Flk-1$^+$-derived aggregates at 72 hr of culture.
(H) Total number of primitive erythroblasts generated from the EryP-CFCs in (G; mean ± SD).
(I) In vivo yolk sac EryP-CFC potential from miR-126$^{+/+}$, miR-126$^{+/-}$, and miR-126$^{-/-}$ embryos (mean ± SEM). n ≥ 3. Student's paired t test *p < 0.05, **p < 0.01. See also Figure S2 and Table S1.

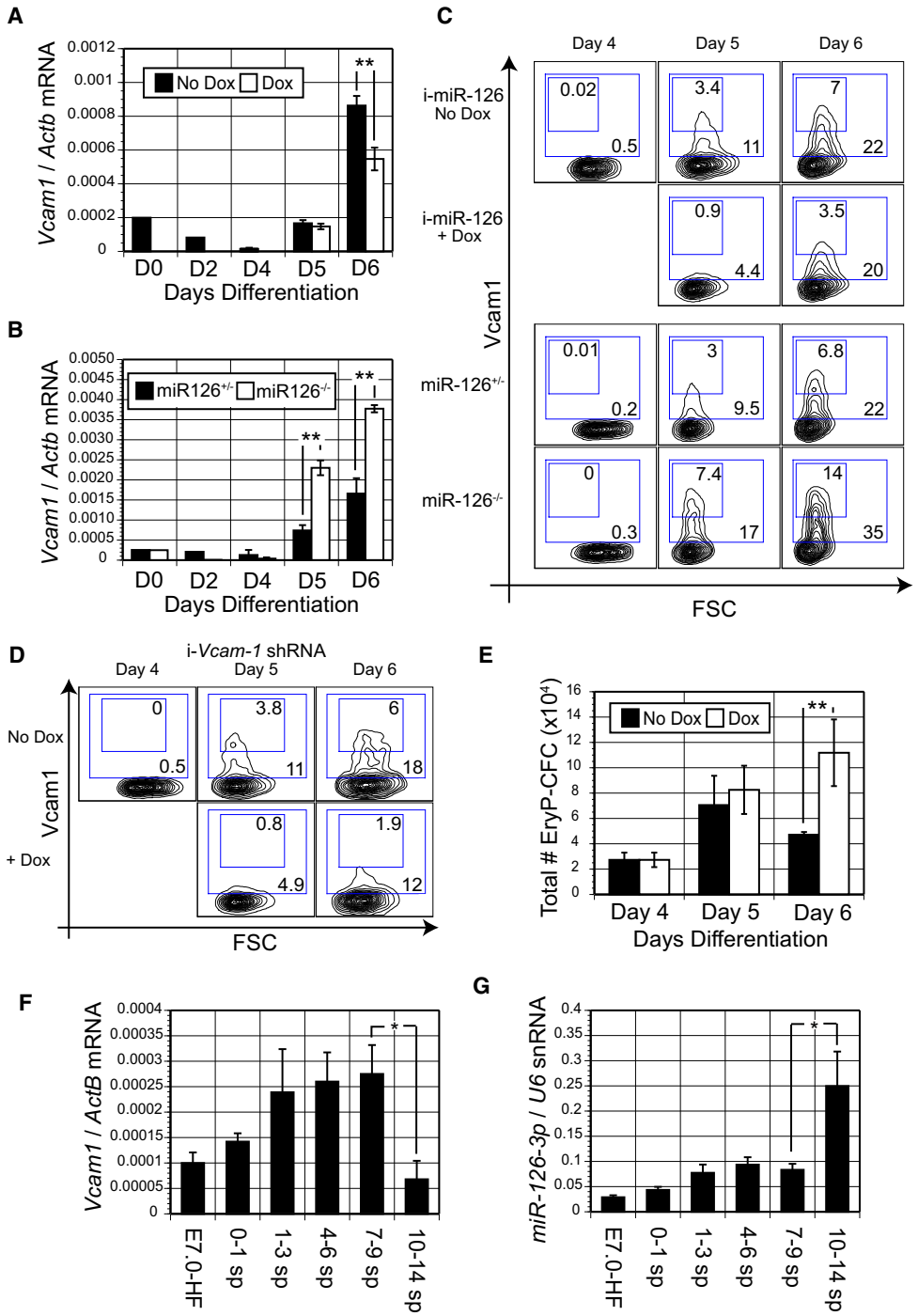

Figure 3. miR-126 Regulates Vcam-1 Expression, Which Negatively Regulates EryP-CFC Development

(A–D) qRT-PCR based expression analyses of *Vcam-1* in miR-126 overexpression (A) and miR-126$^{-/-}$ (B) EBs, as in Figure 2A. Flow cytometric analyses showing the percent of Vcam-1^{+} cells in (C) nonmanipulated, miR-126 induced, miR-126$^{-/-}$ and miR-126$^{+/-}$ EBs at the indicated days of differentiation, and (D) in EBs following expression of a tet-inducible anti-*Vcam-1* shRNA.

(E) Total number of EryP-CFCs in *Vcam-1* shRNA overexpression EBs.

(F and G) qRT-PCR analysis of Vcam-1 (F) and miR-126 (G) in wild-type yolk sacs. n ≥ 3. (mean ± SD) Student's paired t test *p < 0.05, **p < 0.01.

See also Figure S3.

reaggregates, respectively (Figure S3I). No changes in cell growth were observed (data not shown). The strikingly similar outcomes of manipulating either miR-126 or Vcam-1 indicate that *Vcam-1* is not only a relevant target of miR-126-3p, but it also plays a pivotal role in the regulation of primitive erythropoiesis.

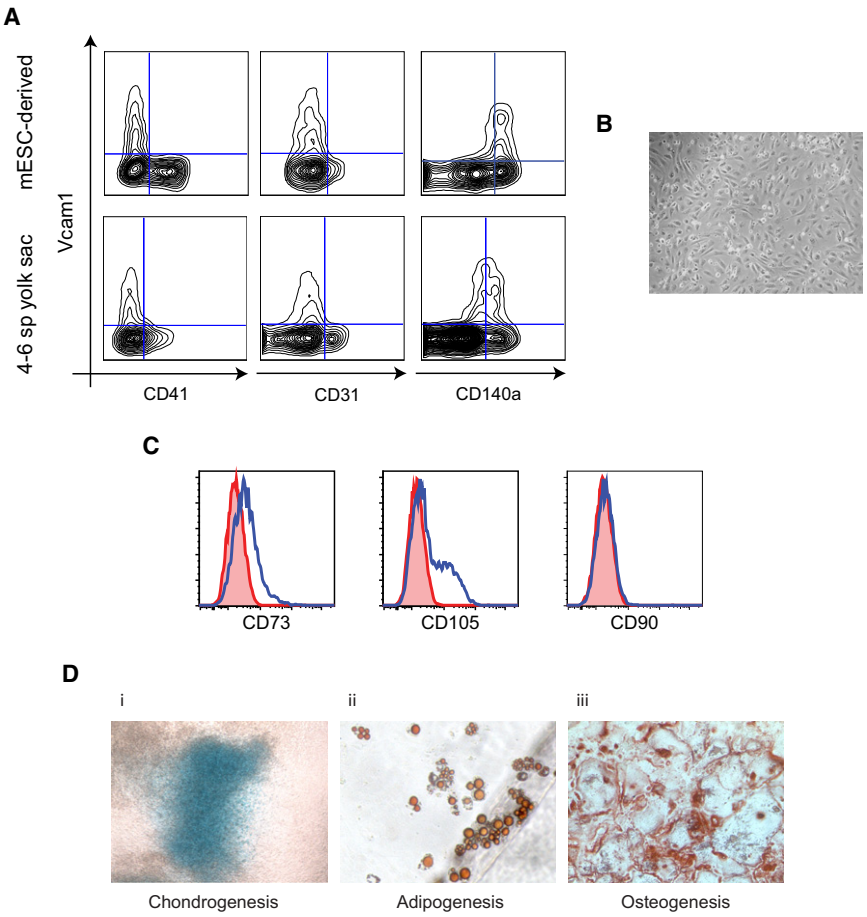

Figure 4. Vcam-1$^+$ Cells Are a Transient Lineage with Mesenchymal Characteristics

(A) Vcam-1 is not expressed on hematopoietic (CD41) or endothelial (CD31) cells in either differentiating EBs (top row) or 4-6 somite yolk sacs (bottom row).

(B) Morphology of FACS-purified mESC-derived Vcam-1$^+$ cells (100×).

(C) Sorted mESC-derived Vcam-1$^+$ cells cultured on gelatin prior to differentiation exhibit low expression of the MSC markers CD73 and CD105 but lack CD90 (blue lines).

(D) Mesenchymal differentiation of mESC-derived Vcam-1$^+$ cells toward chondrocytes (i; alcian blue staining), adipocytes (ii; oil red o staining), and osteocytes (iii; alizarin red staining).

In the developing mouse embryo, Vcam-1 has been found in both the allantois and mesenchyme of the early yolk sac (Downs et al., 2004; Gurtner et al., 1995; Kwee et al., 1995; Sheppard et al., 1994). Analyses of yolk sacs (minus allantois) from different aged embryos revealed a steady increase in Vcam-1 expression from E7.0 to the 7-9 somite pair (sp) stage. The levels dropped sharply between the 7-9 and 10-14 sp stages, a pattern indicative of rapid inhibition of expression (Figure 3F). miR-126-3p expression increased modestly until the 7-9 sp stage and then dramatically at the 10-14 sp stage, coincident with the decline in Vcam-1 expression (Figure 3G). Interestingly, these dynamic changes in miR-126 and Vcam-1 expression occur during the simultaneous loss of adhesion molecules on EryP-CFCs, the termination of their development, and the rapid vasculature remodeling that occurs in the yolk sac at the onset of circulation (reviewed in Baron et al., 2012; Palis et al., 2010).

Flow cytometric analyses of whole EBs and mouse yolk sacs showed that the Vcam-1 population does not express CD41 or CD31 (Figure 4A), indicating that these cells are neither hematopoietic nor endothelial. When isolated from day 6 EBs and cultured on gelatin-coated dishes for 48 hr, the Vcam-1$^+$ cells formed a monolayer that displayed a mesenchymal/fibroblastic morphology (Figure 4B). Analyses of surface markers typically found on mesenchymal cells revealed that, upon sorting and culture in serum, these cells express PDGFRα (Figure 4A) and low levels of CD73. Approximately 20% of the cells acquire CD105$^+$, but none express CD90 (Figure 4C). When assayed under appropriate conditions, the Vcam-1$^+$ cells displayed multi-potent mesenchymal-lineage differentiation capacity, undergoing chondrogenesis, adipogenesis, and osteogenesis (Figure 4D). Taken together, these data demonstrate that the Vcam-1$^+$ cells represent an embryonic mesenchymal cell population that differs from most other mesenchymal cells with respect to expression patterns of surface markers.

To determine if the Vcam-1$^+$-derived population could impact primitive erythroid development in vitro, day 4 EBs containing EryP-CFCs were dissociated, and the cells were cultured on Vcam-1-derived monolayers (Figure 5A). EryP-CFCs were also cocultured with EB-derived CD31$^+$ monolayers as a control. Following 48 hr of culture, the cells were harvested and assayed for EryP-CFC potential. Populations cultured on the Vcam-1$^+$ cells showed a sharp reduction in EryP-CFC potential compared to cells cultured on the CD31$^+$ monolayer or on gelatin alone (Figure 5B), further supporting the interpretation that the Vcam-1$^+$ population negatively regulates primitive erythroid development in the EBs.

Vcam-1-Mediated Repression of EryP-CFC Potential

Molecular analyses revealed that the Vcam-1$^+$ cells express the Notch agonist *Jag-1* and the canonical Wnt antagonist *Dkk-1* (Figures S4A–S4C). As our previous studies have demonstrated, negative regulation of primitive erythropoiesis by both Notch activation and canonical Wnt inhibition (Chen et al., 2008; Cheng et al., 2008; Nostro et al., 2008), we speculated that coculture with Vcam-1$^+$ cells could be regulating EryP potential via these pathways. However, coculture with mESC RBPJ$\kappa^{-/-}$-derived cells (Schroeder et al., 2003), which lack a Notch response, exhibited a similar repression in EryP-CFC potential as RBPJ$\kappa^{+/-}$-derived cells (Figure 5C). Similarly, when 50 ng/ml exogenous Wnt3a was added to cocultures, no rescue of EryP-CFC potential was observed (Figure 5D).

As these known regulators of the primitive erythroid lineage were not involved in this repression, we next investigated

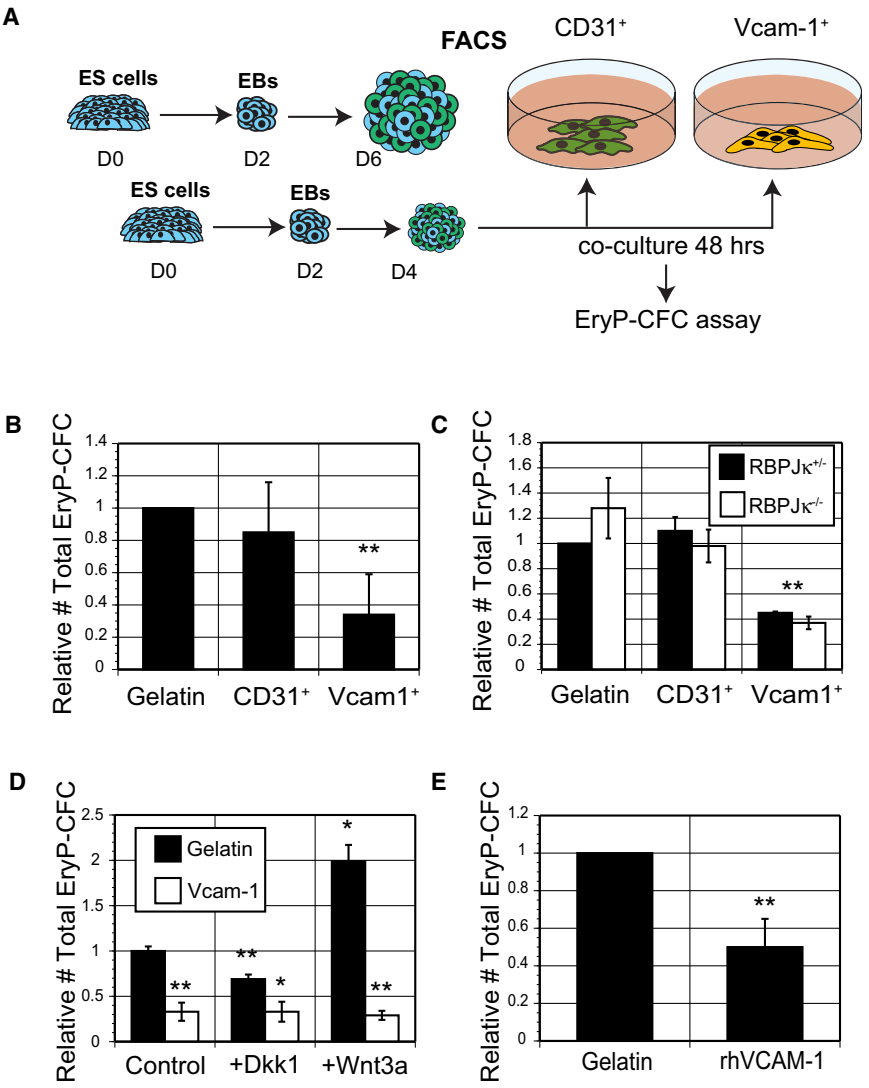

Figure 5. Nonhematopoietic, Nonendothelial Vcam-1$^+$ Cells Negatively Regulate EryP-CFCs in a Cell Nonautonomous Manner

(A) Differentiation scheme depicting the coculture assay used to assess Vcam-1-mediated inhibition of EryP-CFC development. Vcam-1$^+$ and CD31$^+$ cells were isolated from day 6 EBs and cultured for 48 hr on gelatin-coated plates. At this stage, cells from day 4 EBs (source of EryP-CFCs) were added, and the two populations were cultured for an additional 48 hr. Following coculture, the populations were harvested and assayed for EryP-CFC potential.

(B) Relative total number of EryP-CFCs generated following culture of wild-type EB cells on gelatin, CD31$^+$ or Vcam1$^+$ cells.

(C) Relative total number of EryP-CFCs generated from RBPJκ$^{+/-}$ and RBPJκ$^{-/-}$ EB cells coculture as in (B).

(D) Relative total number of EryP-CFCs generated following culture of wild-type EB cells on Vcam1$^+$ in the presence of either Wnt3a (50 ng/ml) or Dkk1 (300 ng/ml).

(E) Relative total number of EryP-CFCs generated following culture of wild-type EB cells on gelatin or rhVCAM-1-coated plasticware. n ≥ 3. (mean ± SD) Student's paired t test *p < 0.05, **p < 0.01. See also Figure S4.

whether Vcam-1 binding to EryP-CFCs is capable of repressing its potential. For these studies, we performed similar coculture assays utilizing other cell lines that express Vcam-1 (Figure S4D) or rhVCAM-1-coated plasticware. In all cases, EryP-CFCs were reduced by ≥50% following Vcam-1$^+$ coculture (Figures 5E and S4E). These observations clearly demonstrate that exposure of primitive erythroid progenitors to Vcam-1 restricts their developmental potential.

Apoptosis was not significantly affected by either miR-126 expression or rhVCAM-1 coculture (data not shown), indicating that the decline in EryP-CFCs is not due to cell death. To determine if interaction with Vcam-1 impacts the rate of maturation of the EryP-CFCs, the cultures were monitored for expression of ßh1-globin and the surface markers CD71 and Ter119. With this analysis, the CD71$^+$Ter119$^-$ fraction contains EryP-CFCs that, following differentiation, give rise to more mature CD71$^+$Ter119$^+$ cells that no longer display clonogenic potential (Socolovsky et al., 2001). Emergence of the more differentiated CD71$^+$Ter119$^+$ fraction was strongly inhibited by either miR-126 overexpression or Vcam-1 silencing (Figure 6A). Conversely, generation of the CD71$^+$Ter119$^+$ population was enhanced when the progenitors were exposed to Vcam-1$^+$ mesenchymal cells or to recombinant Vcam-1. ßh1-globin expression was significantly decreased in EBs following enforced expression of miR-126, whereas it was elevated in miR-126$^{-/-}$ EBs compared to the miR-126$^{+/-}$ EBs (Figure 6B). Together, these results support the interpretation that interaction of EryP-CFCs with Vcam-1 initiates a signaling cascade that accelerates maturation resulting in a loss of detectable progenitors.

SFK Inhibition Restores Vcam-1-Inhibited EryP-CFC Potential

As a first step in identifying potential pathways that mediate the Vcam-1 effect, we treated wild-type EBs with small molecule inhibitors of known effectors of integrin "outside-in" signaling including Src, Fak, Mek, Pi3K, p38, Jak, Jnk, and Caspase to determine which, if any, impact primitive erythropoiesis. Inhibitors were added at day 4 of differentiation, and the EBs were assayed at day 6 for EryP-CFCs. Both the SFK inhibitor PP2 and the MEK inhibitor PD0325901 increased EryP-CFCs in wild-type EBs (Figure 7A). Although a modest increase in EryP-CFCs was observed with the Fak inhibitor, its off-target toxicity (data not shown) may have masked its effect on primitive erythropoiesis. PP2 was able to rescue EryP-CFC potential in miR-126$^{-/-}$ EBs and to increase the frequency of progenitors to levels found in miR-126$^{+/-}$ EBs. Inhibition of MEK, in contrast, did not rescue primitive erythroid

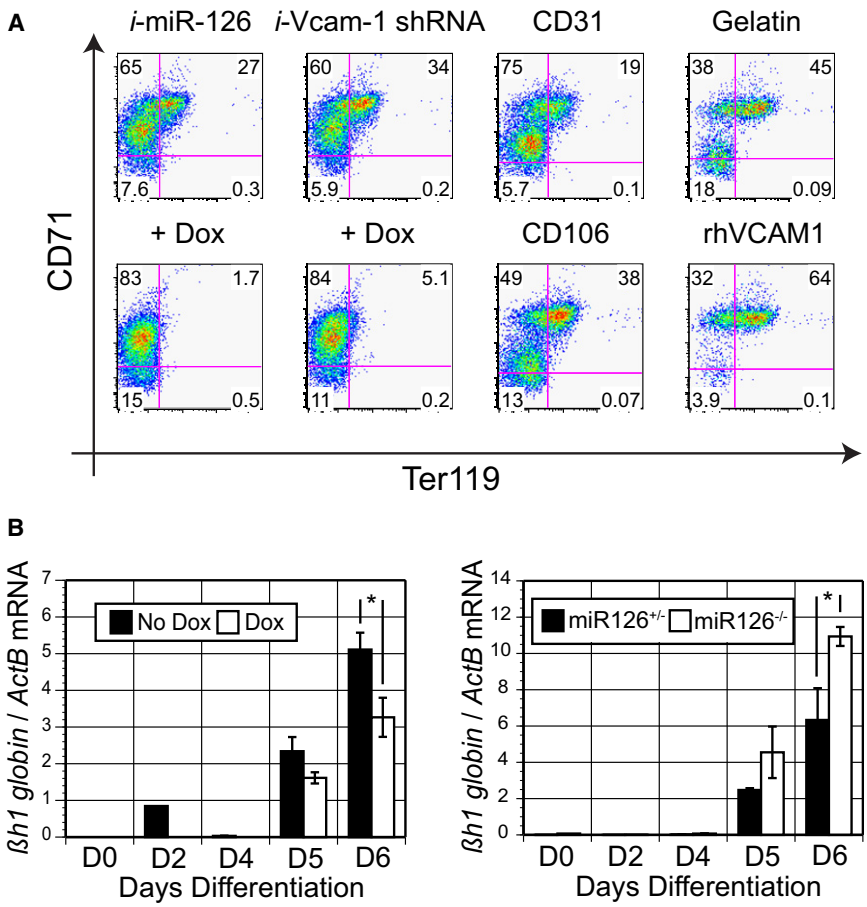

Figure 6. Vcam-1 Exposure to EryP-CFC Causes Maturation

(A) Representative flow cytometric analysis of CD71 and Ter119 in day 6 EBs or 48 hr coculture. Cultures with elevated total Vcam-1$^+$ % have increased Ter119$^+$ cells, indicative of maturation and loss of CFC potential.

(B) qRT-PCR on miR-126 overexpression (left) or miR-126$^{-/-}$ (right) of ßh1-globin. Lower miR-126 expression (thus higher Vcam-1 expression; Figures 3A and 3B) EBs exhibit increased ßh1-globin expression. n = 3. (mean ± SD) Student's paired t test *p < 0.05

potential in these cultures (Figure 7B). Treatment with PP2 significantly reduced Vcam-1 expression in day 6 EBs (Figure S5A), indicating that this may be the reason for the rescue in EryP-CFC in the miR-126$^{-/-}$ EBs. To further investigate this possibility, we added PP2 to rhVCAM-1/EryP-CFC cultures as well as to Vcam-1$^+$ mesenchymal/EryP-CFC cocultures. Under both conditions, the addition of PP2 rescued the Vcam-1-mediated EryP-CFC repression (Figures 7C and 7D). The fact that Vcam-1 levels were not impacted by the PP2 in the coculture (Figure S5B), and that we observed rescue on rhVCAM-1, suggested that the kinase is signaling in the EryP-CFC population.

Analyses of total phosphorylated SFK by western blotting revealed a 25% increase in miR-126$^{-/-}$ EBs compared to miR-126$^{+/-}$ EBs. (Figure 7E), indicating increased activation of this family of kinases in the absence of miR-126. The modest increase in phosphorylated SFK is not unexpected given the broad range of family members expressed in the day 6 EBs (Figure S5C).

DISCUSSION

Primitive erythropoiesis represents a transient hematopoietic program that functions to generate a synchronous wave of primitive erythroblasts that are essential for efficient oxygen transport in the embryo. Primitive erythropoiesis is characterized by the rapid emergence and disappearance of primitive erythroid progenitors within the yolk sac over a 48 hr period in the mouse embryo (Palis et al., 1999). Although the precise timing of EryP-CFC development has been recognized for more than a decade, the signaling pathways that regulate this pattern of erythroid development and the termination of progenitor potential remain poorly understood. In this report, we provide insights into this aspect of primitive erythropoiesis and show the duration of EryP-CFC production is controlled in part by miR-126. Moreover, we show that miR-126 exerts this effect through a pathway that involves the regulation of Vcam-1, a previously published target of this microRNA (Harris et al., 2008), in a cell nonautonomous fashion (model, Figure 7F).

miR-126 has been reported to play a role in hematopoiesis at other stages of development. In zebrafish, miR-126 controls megakaryocyte development through the regulation of c-myb at the stage of the common erythroid/megakaryocyte progenitor (Grabher et al., 2010). As c-myb is not expressed in the primitive erythroid lineage (Tober et al., 2008), these observations indicate that miR-126 can regulate different stages of hematopoiesis through different pathways. Within the human hematopoietic system, miR-126 is expressed in CD34$^+$ human cord blood and mobilized peripheral blood cells (Donahue et al., 2009; Garzon et al., 2006; Gentner et al., 2010; Jin et al., 2008; Shen et al., 2008), suggesting that it may play a role in regulating early stage decisions, possibly at the level of the hematopoietic stem cell. One report has shown that miR-126 is expressed in EBs generated from human ESCs using a serum-based protocol (Huang et al., 2011). In contrast to our findings, however, the authors observed that enforced expression of miR-126 in the whole EB population resulted in marked inhibition of erythropoiesis. PTPN9 was identified as a potential target for this effect, and its enforced expression was able to partially rescue the observed inhibition of erythroid development. We did not detect any changes in *Ptpn9* expression following manipulation of miR-126 in mouse ESC-derived cells (Figures S3C and S3D). The apparent discrepancies between the two studies may be due

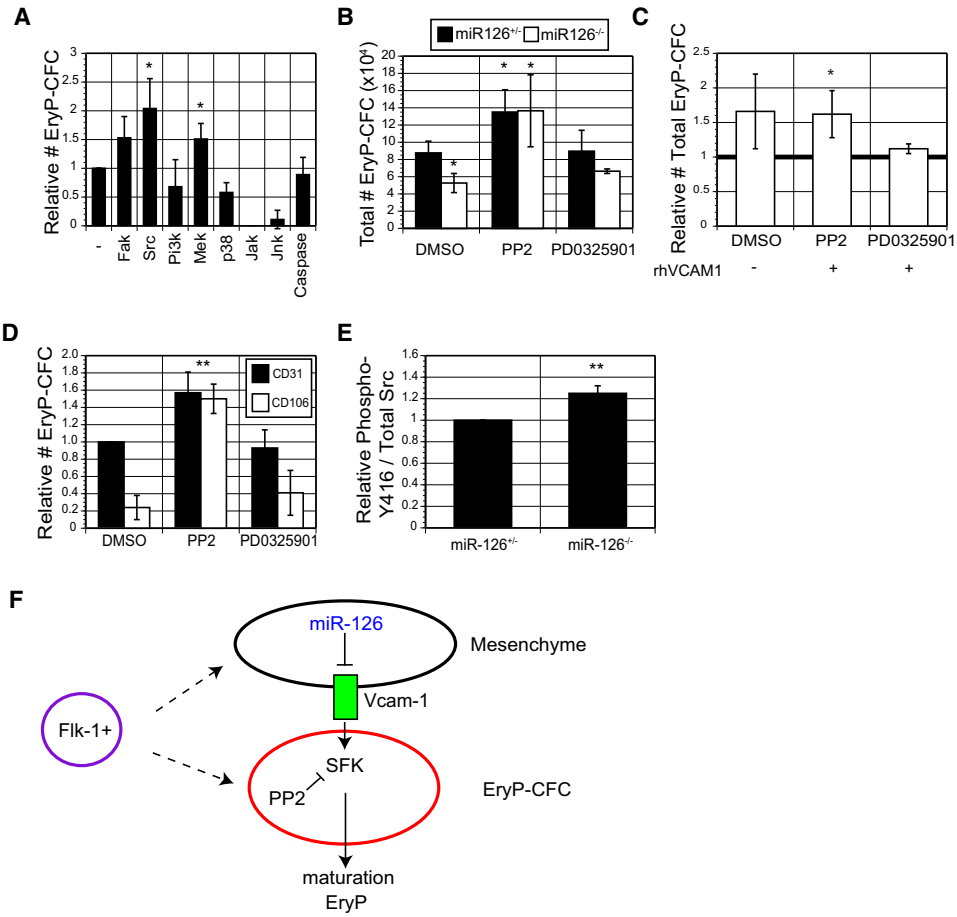

Figure 7. Src-Family Kinase Inhibition Alleviates Vcam-1-Mediated EryP-CFC Repression

(A) Relative total EryP-CFC potential in day 6 EBs treated with various kinase inhibitors for 48 hr.

(B) Relative EryP-CFC potential in miR-126$^{+/-}$ and miR-126$^{-/-}$ day 6 EBs treated with 10 μM PP2 or 1 μM PD0325901 for 48 hr.

(C and D) Relative EryP-CFC potential in 48 hr cocultures on rhVCAM-1 (C) or with CD31^{+} or Vcam-1^{+} cells (D).

(E) Quantification of western blotting for total phosphorylated Y416 Src-family kinase in day 6 EBs. n ≥ 3. (mean ± SD) Student's paired t test *p < 0.05, **p < 0.01.

(F) Model of Vcam-1-mediated EryP-CFC regulation. Flk-1^{+} cells give rise to endothelial (not shown), mesenchymal and hematopoietic progenitors. Over time, the Vcam-1-expressing cells initiate a maturation signal in the EryP-CFC, via a SFK, resulting in loss of CFC potential. miR-126 regulates the expression of Vcam-1, thereby affecting the temporal regulation of the primitive erythroid program.

See also Figure S5.

to differences in the temporal development and regulation of mouse and human primitive erythropoiesis. Future studies utilizing miR-126 antagomirs or knockout human ESC lines, differentiated under serum-free conditions, will likely be required to resolve these differing observations.

Vcam-1 binds several different integrins, including $\alpha_4\beta_1$ (Vla-4) (Chan et al., 1992; Elices et al., 1990), which is expressed on most hematopoietic lineages, including primitive erythroblasts (Fraser et al., 2007). Earlier studies have shown that interaction between Vcam-1 expressed on fetal liver macrophages and Vla-4 expressed by the primitive erythroblasts is required for their enucleation (Isern et al., 2008; Kingsley et al., 2004; McGrath et al., 2008). Our findings indicate that Vcam-1 plays an additional role at an earlier stage of primitive erythroid development where it appears to function on a nonhematopoietic regulatory population, mediating the termination of EryP-CFC development via induction of their maturation (Figure 7F). This interpretation is supported by the observations the period of time during which EryP-CFCs are generated is inversely correlated with the size of the Vcam-1^{+} population (Figure 3) and that coculture of EB-derived cells with rhVCAM-1 results in a reduction of EryP-CFCs (Figure 5E).

The complete rescue of Vcam-1-mediated EryP-CFC repression by Src inhibition strongly suggests that the effect is mediated by activation of a Src family member in the erythroid progenitors. Previous studies have shown that SFKs participate in the regulation of definitive erythropoiesis through a variety of mechanisms, such as regulation of EPOR, EGFR, and integrin signaling (reviewed in Ingley et al., 2004; Richmond et al., 2005). Lyn kinase, in particular, has been reported to play a significant role in erythropoiesis, with Lyn$^{-/-}$ mice exhibiting a striking increase in spleen and bone marrow-derived CFU-E

(Harder et al., 2004). Our findings extend a regulatory role of SFKs to the primitive erythroid lineage and, specifically, to the termination of the program. Current studies are aimed at determining which family member is responsible for mediating this effect.

The observation that the Flk-1$^+$ hemangioblast population is able to generate both the Vcam-1$^+$ regulatory cells and the primitive erythroid lineage suggests that they may be derived from a common progenitor. While the exact nature of the Vcam-1$^+$ population remains unknown, our findings to date indicate it represents a mesenchymal population capable of trilineage differentiation. The surface marker phenotype of the mESC-derived Vcam-1$^+$ MSCs is distinct from those generated from adult tissues, suggesting they may represent a unique population that functions transiently in the yolk sac, providing a regulatory niche to trigger erythroid maturation and termination of progenitor development.

The dynamics of *Vcam-1* expression in the developing yolk sac (Figure 3F) and the presence of a distinct Vcam-1$^+$ population in 4-6 sp pair yolk sacs is consistent with a role for this molecule in regulating primitive erythropoiesis in vivo. EryP-CFC development in the yolk sac initiates at E7.0 and persists until E8.5 (Palis et al., 1999). The presence of Vcam-1$^+$ cells in the yolk sac during late stages of primitive erythropoiesis supports the interpretation that they function to regulate the duration of the progenitor development in vivo, as they do in vitro. The dramatic drop in levels of *Vcam-1* expression over a matter of hours between the 7-9 sp and 10-14 sp stages of development indicates that the MSC population, or at least *Vcam-1* expression, is tightly controlled at this stage. The sharp spike in miR-126-3p at this stage supports the interpretation that its expression is responsible for this rapid decline in Vcam-1. miR-126-3p is expressed during the primitive erythroid stage of yolk sac development, at levels that may function to balance the size of the MSC population or the amount of Vcam-1 expressed. The observation that miR-126-3p null embryos have reduced numbers of EryP-CFCs demonstrates that these levels of expression are functional and important for regulating primitive erythroid development in vivo. Given the rapid temporal changes in *Vcam-1* expression and limited access to tissues at this stage of development, observations of a direct correlation between miR-126-3p and Vcam-1 expression in the mutant embryos is not possible. The complimentary findings from the mESC model recapitulating primitive erythropoiesis in vivo highlight the power of this in vitro system for studying lineage specification and once again demonstrate that developmental events in vitro accurately recapitulate those in the early embryo.

In summary, the findings in this study provide evidence of a pathway that regulates the terminal stages of primitive erythroid progenitor development in the mESC model as well as in the mouse embryo yolk sac. The identification of a Vcam-1$^+$ population that is regulated in part by miR-126 uncovers a cell nonautonomous pathway for controlling primitive erythropoiesis. With access to this regulatory population, it will be possible to study the mechanisms through which it mediates this effect and determine if it plays a larger role in the transition from the primitive to definitive hematopoietic programs in ESC-derived differentiation cultures.

EXPERIMENTAL PROCEDURES

ESC Maintenance and Differentiation

All mESC lines were maintained and differentiated under feeder-free, serum-free conditions (Gadue et al., 2006) as described in Supplemental Experimental Procedures.

EryP-CFC Assays

Primitive erythroid progenitor assays were performed as previously described (Nostro et al., 2008; Palis et al., 1999). Differentiation reaggregates were trypsinized to single-cells and plated in IMDM/methylcellulose containing 10% plasma-derived serum, 5% PFHM-II, 300 μg/ml transferrin, 2U/ml EPO, 2 mM glutamine, 50 μg/ml ascorbic acid, and 4.5 × 10^{-4} M 1-thioglycerol. Colonies (EryP-CFC) were scored 5 days after plating. Values presented represent averages across three or more replicates, ± SD. Student's paired t test and ANOVA statistical analysis were used to determine significance ($p < 0.05$) in different colony-forming potential between groups.

Coculture EryP-CFC Assay

Sorted Vcam-1$^+$ cells from day 6 differentiation cultures were plated onto gelatin-coated 96-well plates at 20,000 cells/well in SFD containing 25 ng/ml hPDGF-BB and 10 ng/ml hFGF-2. Sorted CD31$^+$ cells from the same cultures were plated in 50 ng/ml hVEGF and 10 ng/ml hFGF-2. Recombinant human Vcam-1 (10 μg/ml; BD Biosciences) was coated on 96-well plates for 1 hr prior to cell seeding. Cells were cultured for 48 hr, then washed in IMDM and overlayed with 50,000 day 4 EB cells in SFD with 5 ng/ml hVEGF. Cocultures were harvested (suspension and adherent fractions) 48 hr later and assayed for EryP-CFC activity.

Kinase Inhibitor EryP-CFC Assays

mESC were differentiated and assayed as above, but small molecule inhibitors were added at day 4 of differentiation in place of DOX. FAK inhibitor PF573228 (1 μM), Src inhibitor PP2 (10 μM), PI3K inhibitor LY294002 (20 μM), MEK inhibitor PD0325901 (1 μM), p38 inhibitor SB203580 (10 μM), JAK inhibitor AG490 (1 μM) JNK inhibitor SP600125 (10 μM), and caspase inhibitor Z-VAD-FMK (10 μM) were obtained from Tocris.

In Vivo Analysis

Embryos from timed matings were harvested from E7.0-8.5. Yolk sacs were dissected and the allantois was removed and then dissociated by trypsinization for 5 min. Resultant cells were analyzed by flow cytometry, harvested for qRT-PCR, or plated in methylcellulose for EryP-CFC analysis. EryP-CFC values presented represent average ±SEM. ANOVA statistical analysis was used to determine significance ($p < 0.05$) in different colony-forming potential between groups. The embryo proper was used for genotyping miR-126 status. Work involving mouse tissue collection and analysis was carried out in accordance with and approved through the Animal Care Committee at the University Health Network.

Microarray for MicroRNA

MicroRNA expression was analyzed by microarray as previously described (Thomson et al., 2004). Briefly, 5 μg total RNA was labeled with Cy3 and hybridized to a custom oligonucleotide microarray. Intensity values were filtered to remove values below 2× background and the global median center was normalized. Hierarchical clustering was performed. A clade of the full heat map is shown in Figure S1B. Microarray data can be accessed at the NCBI GEO database with accession number GSE37727.

Mesenchymal Lineage Potential Assays

Sorted Vcam-1$^+$ cells were plated onto gelatin-coated 96-well plates at serial dilutions in SFD. Osteoblastic differentiation was induced using the StemPro Osteogenesis Differentiation kit (Life Technologies) for 21 days. Adipocyte differentiation was induced using the Mesenchymal Adipogenesis kit (Millipore) for 21 days. Chondrocyte differentiation was induced by the addition of 100 μg/ml BMP4 and 10 μg/ml bFGF for 9 days. Cells were fixed in 4% paraformaldehyde for 20 min at room temperature and then stained with Alizarin Red (osteogenesis), Oil Red O (adipogenesis), or Alcian Blue (chondrogenesis).

FACS Analyses and Cell Sorting

EBs were dissociated to single cells with trypsin and incubated in IMDM+0.02% BSA (Sigma) with antibodies for the following surface antigens: anti-mouse VEGFR2-biotin, anti-mouse CD31-PE or -APC, anti-mouse CD41-FITC or -APC, anti-mouse Vcam-1-biotin, anti-mouse CD73-PE, anti-mouse CD105-APC, anti-mouse CD90-Pacific Blue, and streptavidin-PE or -APC (BD). Cells were acquired with an LSR II (BD) or sorted with using a FACSAriaII (SickKids, UHN Flow Cytometry Facility, Toronto, ON, Canada). Analysis was performed with FlowJo software (Tree Star, Inc.).

SUPPLEMENTAL INFORMATION

Supplemental Information includes five figures, one table, and Supplemental Experimental Procedures and can be found with this article online at http://dx.doi.org/10.1016/j.devcel.2012.05.021.

ACKNOWLEDGMENTS

This work was supported by a CIHR Operating grant (MOP93569). C.M.S. was supported by a McMurrich Post-Doctoral Fellowship at the McEwen Centre for Regenerative Medicine, Toronto, ON, Canada. Antagomirs were provided by Dr. E. Lechman (University of Toronto). We thank R. Banh and R. Marcotte for assistance with western blotting and members of the Keller laboratory for critical reading of the manuscript. E.N.O. is cofounder and member of the SAB of Miragen Therapeutics, a biotech company developing microRNA-based therapeutics for cardiovascular disease. G.K. is on the SAB of Vistagen Therapeutics and holds stock in the company; he is also a consultant for StemGent.

Received: February 11, 2011
Revised: March 27, 2012
Accepted: May 29, 2012
Published online: June 28, 2012

REFERENCES

Baron, M.H., Isern, J., and Fraser, S.T. (2012). The embryonic origins of erythropoiesis in mammals. Blood *119*, 4828–4837.

Bartel, D.P. (2004). MicroRNAs: genomics, biogenesis, mechanism, and function. Cell *116*, 281–297.

Bernstein, E., Kim, S.Y., Carmell, M.A., Murchison, E.P., Alcorn, H., Li, M.Z., Mills, A.A., Elledge, S.J., Anderson, K.V., and Hannon, G.J. (2003). Dicer is essential for mouse development. Nat. Genet. *35*, 215–217.

Chan, B.M., Elices, M.J., Murphy, E., and Hemler, M.E. (1992). Adhesion to vascular cell adhesion molecule 1 and fibronectin. Comparison of alpha 4 beta 1 (VLA-4) and alpha 4 beta 7 on the human B cell line JY. J. Biol. Chem. *267*, 8366–8370.

Chen, V.C., Stull, R., Joo, D., Cheng, X., and Keller, G. (2008). Notch signaling respecifies the hemangioblast to a cardiac fate. Nat. Biotechnol. *26*, 1169–1178.

Cheng, X., Huber, T.L., Chen, V.C., Gadue, P., and Keller, G.M. (2008). Numb mediates the interaction between Wnt and Notch to modulate primitive erythropoietic specification from the hemangioblast. Development *135*, 3447–3458.

Choi, K., Kennedy, M., Kazarov, A., Papadimitriou, J.C., and Keller, G. (1998). A common precursor for hematopoietic and endothelial cells. Development *125*, 725–732.

Donahue, R.E., Jin, P., Bonifacino, A.C., Metzger, M.E., Ren, J., Wang, E., and Stroncek, D.F. (2009). Plerixafor (AMD3100) and granulocyte colony-stimulating factor (G-CSF) mobilize different CD34+ cell populations based on global gene and microRNA expression signatures. Blood *114*, 2530–2541.

Downs, K.M., Hellman, E.R., McHugh, J., Barrickman, K., and Inman, K.E. (2004). Investigation into a role for the primitive streak in development of the murine allantois. Development *131*, 37–55.

Elices, M.J., Osborn, L., Takada, Y., Crouse, C., Luhowskyj, S., Hemler, M.E., and Lobb, R.R. (1990). VCAM-1 on activated endothelium interacts with the leukocyte integrin VLA-4 at a site distinct from the VLA-4/fibronectin binding site. Cell *60*, 577–584.

Ferkowicz, M.J., and Yoder, M.C. (2005). Blood island formation: longstanding observations and modern interpretations. Exp. Hematol. *33*, 1041–1047.

Fish, J.E., Santoro, M.M., Morton, S.U., Yu, S., Yeh, R.F., Wythe, J.D., Ivey, K.N., Bruneau, B.G., Stainier, D.Y., and Srivastava, D. (2008). miR-126 regulates angiogenic signaling and vascular integrity. Dev. Cell *15*, 272–284.

Fraser, S.T., Isern, J., and Baron, M.H. (2007). Maturation and enucleation of primitive erythroblasts during mouse embryogenesis is accompanied by changes in cell-surface antigen expression. Blood *109*, 343–352.

Gadue, P., Huber, T.L., Paddison, P.J., and Keller, G.M. (2006). Wnt and TGF-beta signaling are required for the induction of an *in vitro* model of primitive streak formation using embryonic stem cells. Proc. Natl. Acad. Sci. USA *103*, 16806–16811.

Garzon, R., Pichiorri, F., Palumbo, T., Iuliano, R., Cimmino, A., Aqeilan, R., Volinia, S., Bhatt, D., Alder, H., Marcucci, G., et al. (2006). MicroRNA fingerprints during human megakaryocytopoiesis. Proc. Natl. Acad. Sci. USA *103*, 5078–5083.

Gentner, B., Visigalli, I., Hiramatsu, H., Lechman, E., Ungari, S., Giustacchini, A., Schira, G., Amendola, M., Quattrini, A., Martino, S., et al. (2010). Identification of hematopoietic stem cell-specific miRNAs enables gene therapy of globoid cell leukodystrophy. Sci. Transl. Med. *2*, 58ra84.

Grabher, C., Payne, E.M., Johnston, A.B., Bolli, N., Lechman, E., Dick, J.E., Kanki, J.P., and Look, A.T. (2010). Zebrafish microRNA-126 determines hematopoietic cell fate through c-Myb. Leukemia *25*, 506–514.

Griffiths-Jones, S. (2004). The microRNA Registry. Nucleic Acids Res. *32* (Database issue), D109–D111.

Gurtner, G.C., Davis, V., Li, H., McCoy, M.J., Sharpe, A., and Cybulsky, M.I. (1995). Targeted disruption of the murine VCAM1 gene: essential role of VCAM-1 in chorioallantoic fusion and placentation. Genes Dev. *9*, 1–14.

Harder, K.W., Quilici, C., Naik, E., Inglese, M., Kountouri, N., Turner, A., Zlatic, K., Tarlinton, D.M., and Hibbs, M.L. (2004). Perturbed myelo/erythropoiesis in Lyn-deficient mice is similar to that in mice lacking the inhibitory phosphatases SHP-1 and SHIP-1. Blood *104*, 3901–3910.

Harris, T.A., Yamakuchi, M., Ferlito, M., Mendell, J.T., and Lowenstein, C.J. (2008). MicroRNA-126 regulates endothelial expression of vascular cell adhesion molecule 1. Proc. Natl. Acad. Sci. USA *105*, 1516–1521.

Harris, T.A., Yamakuchi, M., Kondo, M., Oettgen, P., and Lowenstein, C.J. (2010). Ets-1 and Ets-2 regulate the expression of microRNA-126 in endothelial cells. Arterioscler. Thromb. Vasc. Biol. *30*, 1990–1997.

Huang, X., Gschweng, E., Van Handel, B., Cheng, D., Mikkola, H.K., and Witte, O.N. (2011). Regulated expression of microRNAs-126/126* inhibits erythropoiesis from human embryonic stem cells. Blood *117*, 2157–2165.

Huber, T.L., Kouskoff, V., Fehling, H.J., Palis, J., and Keller, G. (2004). Haemangioblast commitment is initiated in the primitive streak of the mouse embryo. Nature *432*, 625–630.

Ingley, E., Tilbrook, P.A., and Klinken, S.P. (2004). New insights into the regulation of erythroid cells. IUBMB Life *56*, 177–184.

Isern, J., Fraser, S.T., He, Z., and Baron, M.H. (2008). The fetal liver is a niche for maturation of primitive erythroid cells. Proc. Natl. Acad. Sci. USA *105*, 6662–6667.

Ivey, K.N., and Srivastava, D. (2010). MicroRNAs as regulators of differentiation and cell fate decisions. Cell Stem Cell *7*, 36–41.

Jin, P., Wang, E., Ren, J., Childs, R., Shin, J.W., Khuu, H., Marincola, F.M., and Stroncek, D.F. (2008). Differentiation of two types of mobilized peripheral blood stem cells by microRNA and cDNA expression analysis. J. Transl. Med. *6*, 39.

Kennedy, M., Firpo, M., Choi, K., Wall, C., Robertson, S., Kabrun, N., and Keller, G. (1997). A common precursor for primitive erythropoiesis and definitive haematopoiesis. Nature *386*, 488–493.

Kingsley, P.D., Malik, J., Fantauzzo, K.A., and Palis, J. (2004). Yolk sac-derived primitive erythroblasts enucleate during mammalian embryogenesis. Blood *104*, 19–25.

Kloosterman, W.P., and Plasterk, R.H. (2006). The diverse functions of microRNAs in animal development and disease. Dev. Cell *11*, 441–450.

Krützfeldt, J., Rajewsky, N., Braich, R., Rajeev, K.G., Tuschl, T., Manoharan, M., and Stoffel, M. (2005). Silencing of microRNAs *in vivo* with 'antagomirs'. Nature *438*, 685–689.

Kuehbacher, A., Urbich, C., Zeiher, A.M., and Dimmeler, S. (2007). Role of Dicer and Drosha for endothelial microRNA expression and angiogenesis. Circ. Res. *101*, 59–68.

Kwee, L., Baldwin, H.S., Shen, H.M., Stewart, C.L., Buck, C., Buck, C.A., and Labow, M.A. (1995). Defective development of the embryonic and extraembryonic circulatory systems in vascular cell adhesion molecule (VCAM-1) deficient mice. Development *121*, 489–503.

Kyba, M., Perlingeiro, R.C., and Daley, G.Q. (2002). HoxB4 confers definitive lymphoid-myeloid engraftment potential on embryonic stem cell and yolk sac hematopoietic progenitors. Cell *109*, 29–37.

Lagos-Quintana, M., Rauhut, R., Yalcin, A., Meyer, J., Lendeckel, W., and Tuschl, T. (2002). Identification of tissue-specific microRNAs from mouse. Curr. Biol. *12*, 735–739.

Landgraf, P., Rusu, M., Sheridan, R., Sewer, A., Iovino, N., Aravin, A., Pfeffer, S., Rice, A., Kamphorst, A.O., Landthaler, M., et al. (2007). A mammalian microRNA expression atlas based on small RNA library sequencing. Cell *129*, 1401–1414.

Li, Z., Lu, J., Sun, M., Mi, S., Zhang, H., Luo, R.T., Chen, P., Wang, Y., Yan, M., Qian, Z., et al. (2008). Distinct microRNA expression profiles in acute myeloid leukemia with common translocations. Proc. Natl. Acad. Sci. USA *105*, 15535–15540.

Luche, H., Weber, O., Nageswara Rao, T., Blum, C., and Fehling, H.J. (2007). Faithful activation of an extra-bright red fluorescent protein in "knock-in" Cre-reporter mice ideally suited for lineage tracing studies. Eur. J. Immunol. *37*, 43–53.

Mansfield, J.H., Harfe, B.D., Nissen, R., Obenauer, J., Srineel, J., Chaudhuri, A., Farzan-Kashani, R., Zuker, M., Pasquinelli, A.E., Ruvkun, G., et al. (2004). MicroRNA-responsive 'sensor' transgenes uncover Hox-like and other developmentally regulated patterns of vertebrate microRNA expression. Nat. Genet. *36*, 1079–1083.

McGrath, K.E., Kingsley, P.D., Koniski, A.D., Porter, R.L., Bushnell, T.P., and Palis, J. (2008). Enucleation of primitive erythroid cells generates a transient population of "pyrenocytes" in the mammalian fetus. Blood *111*, 2409–2417.

Nakano, T., Kodama, H., and Honjo, T. (1996). In vitro development of primitive and definitive erythrocytes from different precursors. Science *272*, 722–724.

Nicoli, S., Standley, C., Walker, P., Hurlstone, A., Fogarty, K.E., and Lawson, N.D. (2010). MicroRNA-mediated integration of haemodynamics and Vegf signalling during angiogenesis. Nature *464*, 1196–1200.

Nishikawa, S.I., Nishikawa, S., Hirashima, M., Matsuyoshi, N., and Kodama, H. (1998). Progressive lineage analysis by cell sorting and culture identifies FLK1+VE-cadherin+ cells at a diverging point of endothelial and hemopoietic lineages. Development *125*, 1747–1757.

Nostro, M.C., Cheng, X., Keller, G.M., and Gadue, P. (2008). Wnt, activin, and BMP signaling regulate distinct stages in the developmental pathway from embryonic stem cells to blood. Cell Stem Cell *2*, 60–71.

O'Connell, R.M., Chaudhuri, A.A., Rao, D.S., Gibson, W.S., Balazs, A.B., and Baltimore, D. (2010). MicroRNAs enriched in hematopoietic stem cells differentially regulate long-term hematopoietic output. Proc. Natl. Acad. Sci. USA *107*, 14235–14240.

Palis, J., Robertson, S., Kennedy, M., Wall, C., and Keller, G. (1999). Development of erythroid and myeloid progenitors in the yolk sac and embryo proper of the mouse. Development *126*, 5073–5084.

Palis, J., Malik, J., McGrath, K.E., and Kingsley, P.D. (2010). Primitive erythropoiesis in the mammalian embryo. Int. J. Dev. Biol. *54*, 1011–1018.

Pearson, S., Sroczynska, P., Lacaud, G., and Kouskoff, V. (2008). The stepwise specification of embryonic stem cells to hematopoietic fate is driven by sequential exposure to Bmp4, activin A, bFGF and VEGF. Development *135*, 1525–1535.

Poliseno, L., Tuccoli, A., Mariani, L., Evangelista, M., Citti, L., Woods, K., Mercatanti, A., Hammond, S., and Rainaldi, G. (2006). MicroRNAs modulate the angiogenic properties of HUVECs. Blood *108*, 3068–3071.

Richmond, T.D., Chohan, M., and Barber, D.L. (2005). Turning cells red: signal transduction mediated by erythropoietin. Trends Cell Biol. *15*, 146–155.

Schroeder, T., Kohlhof, H., Rieber, N., and Just, U. (2003). Notch signaling induces multilineage myeloid differentiation and up-regulates PU.1 expression. J. Immunol. *170*, 5538–5548.

Shen, W.F., Hu, Y.L., Uttarwar, L., Passegue, E., and Largman, C. (2008). MicroRNA-126 regulates HOXA9 by binding to the homeobox. Mol. Cell. Biol. *28*, 4609–4619.

Sheppard, A.M., Onken, M.D., Rosen, G.D., Noakes, P.G., and Dean, D.C. (1994). Expanding roles for alpha 4 integrin and its ligands in development. Cell Adhes. Commun. *2*, 27–43.

Socolovsky, M., Nam, H., Fleming, M.D., Haase, V.H., Brugnara, C., and Lodish, H.F. (2001). Ineffective erythropoiesis in Stat5a(-/-)5b(-/-) mice due to decreased survival of early erythroblasts. Blood *98*, 3261–3273.

Thomson, J.M., Parker, J., Perou, C.M., and Hammond, S.M. (2004). A custom microarray platform for analysis of microRNA gene expression. Nat. Methods *1*, 47–53.

Tober, J., McGrath, K.E., and Palis, J. (2008). Primitive erythropoiesis and megakaryopoiesis in the yolk sac are independent of c-myb. Blood *111*, 2636–2639.

Wang, S., Aurora, A.B., Johnson, B.A., Qi, X., McAnally, J., Hill, J.A., Richardson, J.A., Bassel-Duby, R., and Olson, E.N. (2008). The endothelial-specific microRNA miR-126 governs vascular integrity and angiogenesis. Dev. Cell *15*, 261–271.

Wienholds, E., Kloosterman, W.P., Miska, E., Alvarez-Saavedra, E., Berezikov, E., de Bruijn, E., Horvitz, H.R., Kauppinen, S., and Plasterk, R.H. (2005). MicroRNA expression in zebrafish embryonic development. Science *309*, 310–311.

Yang, G.H., Wang, F., Yu, J., Wang, X.S., Yuan, J.Y., and Zhang, J.W. (2009). MicroRNAs are involved in erythroid differentiation control. J. Cell. Biochem. *107*, 548–556.

Zhao, Y., Samal, E., and Srivastava, D. (2005). Serum response factor regulates a muscle-specific microRNA that targets Hand2 during cardiogenesis. Nature *436*, 214–220.